

Robotic Monitoring of Colorimetric Leaf Sensors for Precision Agriculture

Malakhi Hopkins^{*,1} Alice Kate Li^{*,1} Shobhita Kramadhati^{*,1} Jackson Arnold²
 Akhila Mallavarapu¹ Chavez Lawrence¹ Varun Murali¹
 Sanjeev J. Koppal^{2,3} Cherie Kagan¹ Vijay Kumar¹

Abstract—Current remote sensing technologies that measure crop health *e.g.* RGB, multispectral, hyperspectral, and LiDAR, are indirect, and cannot capture plant stress indicators directly. Instead, low-cost leaf sensors that directly interface with the crop surface present an opportunity to advance real-time direct monitoring. To this end, we co-design a sensor-detector system, where the sensor is a novel colorimetric leaf sensor that directly measures crop health in a precision agriculture setting, and the detector autonomously obtains optical signals from these leaf sensors. This system integrates a ground robot platform with an on-board monocular RGB camera and object detector to localize the leaf sensor, and a hyperspectral camera with motorized mirror and an on-board halogen light to acquire a hyperspectral reflectance image of the leaf sensor, from which a spectral response characterizing crop health can be extracted. We show a successful demonstration of our co-designed system operating in outdoor environments, obtaining laboratory-grade spectrometer measurements. The system is demonstrated in row-crop environments both indoors and outdoors where it is able to autonomously navigate, locate and obtain a hyperspectral image of all leaf sensors present, and retrieve interpretable spectral resonance from leaf sensors.

I. INTRODUCTION

With the increasing global population, precision farming is necessary to meet increased food demands and reduce food waste. Mobile robots with on-board sensing are well-suited for precision agriculture tasks, as they can persistently monitor crops at the plant level and provide mitigation strategies depending on crop conditions. However, to better understand and improve crop growth, we must introduce new technologies in precision farming that can measure plant stress indicators more accurately. More precise information will allow farmers to consistently provide optimal growing conditions and maximize yield.

Current remote sensing technologies used in precision agriculture are limiting as they provide information that indirectly measure crop health traits. Such sensing technology includes RGB, multispectral, hyperspectral, and LiDAR imaging on either aerial or ground robot platforms [1].

Accepted to the Novel Approaches for Precision Agriculture and Forestry with Autonomous Robots IEEE ICRA Workshop - 2025

^{*}Equal contribution.

¹ GRASP Laboratory, University of Pennsylvania, Pennsylvania, USA

² University of Florida, Florida, USA

³ Amazon Robotics. Sanjeev J. Koppal holds concurrent appointments as an Associate Professor of ECE at the University of Florida and as an Amazon Scholar at Amazon Robotics. This paper describes work performed at the University of Florida and is not associated with Amazon.

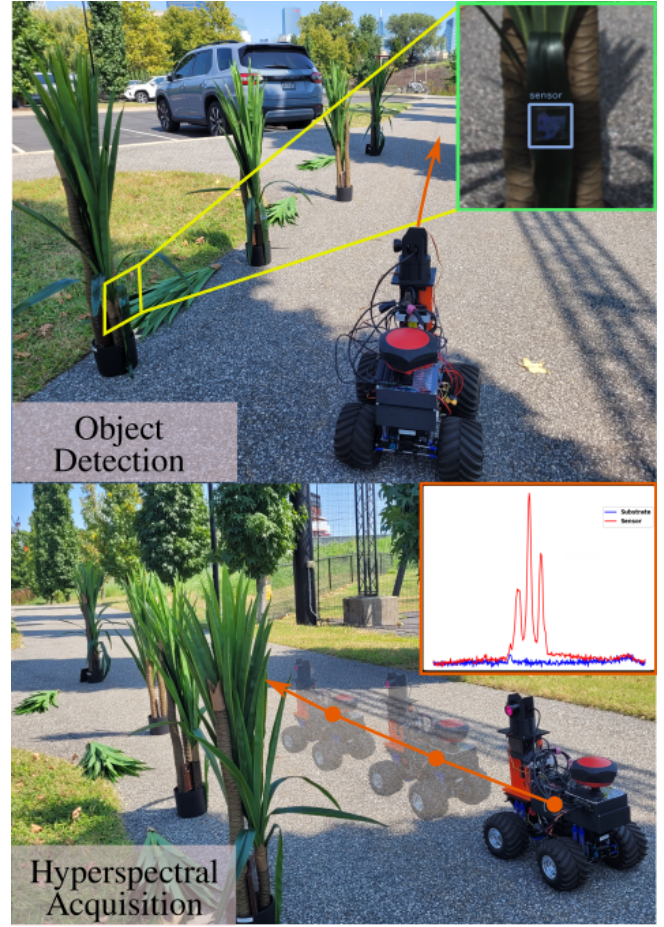


Fig. 1: Our ground robot platform, BEAST, is equipped with visual-inertial odometry-based localization and an RGB monocular camera to localize colorimetric leaf sensors mounted on plants. Hyperspectral images and spectra of the leaf sensors are acquired via an on-board hyperspectral camera and a motorized mirror control system.

These systems measure crop or soil reflectance and canopy structure. The data collected with these methods serve as a proxy for crop health traits.

More advanced technologies, on the other hand, are able to acquire data that indicate plant stress more directly. Plant stress can be estimated by monitoring leaf moisture and temperature, soil pH and nitrogen content, to name a few. Low-cost, distributable sensors are capable of measuring these

plant stress indicators and present an opportunity to advance real-time monitoring and spatial mapping of crop health traits [2]. To this end, we co-design a sensor-detector system based on colorimetric leaf sensors that directly measure plant stress indicators and passively communicate this information through optical signals detectable by a robot with on-board imaging.

The contributions of this work include:

- 1) a passive, optical-metasurface-based, colorimetric leaf sensor that can respond to changes in the local environmental variables that affect crop health whose resonance spectrum we measure outdoors;
- 2) the design and build of a low-cost, lightweight ground robot platform, BEAST, integrated with a novel hyperspectral imaging system for detecting and measuring deployed leaf sensors; and
- 3) a pipeline that performs colorimetric leaf sensor detection from online RGB images, visual servoing for hyperspectral reflectance imaging with a hyperspectral camera and motorized mirror.

II. RELATED WORK

The colorimetric leaf sensor we propose for the co-designed sensor-detector system is a metasurface refractive index sensor. Recently, there has been much interest in the application of nanophotonics for biosensing. These nanostructured metasurfaces exploit various optical phenomena such as metallic surface plasmon resonances (SPR) and dielectric Mie resonances as their sensing mechanism, since the spectral positions of the reflectance spectrum peaks, or resonances, are dependent upon the refractive index of the medium surrounding the metasurface [3], [4]. The colorimetric leaf sensor, as reported in [5], is novel in its use of solution-processible, dielectric nanocrystal inks which enable low-cost, high-throughput scalable fabrication. The nanostructured metasurface can be integrated with an adaptive polymer that is responsive to environmental conditions such as moisture and temperature, making the sensor particularly suitable for passive, continuous monitoring of crop health. Conventional monitoring of leaf transpiration and moisture involves bulky, powered electronics such as porometers, as discussed in [6]. As [5] shows, these passive metasurface-based sensors are transparent and ultra-compact and lightweight, making them suitable as leaf sensors, as they would not interfere with crop growth. For these novel colorimetric leaf sensors deployed en-masse in an agricultural setting, a suitable detector, such as a robotic imaging system must then be developed to successfully detect and extract the spectral resonance from them.

While our work involves detecting transparent leaf sensors in an agricultural environment, existing precision agriculture platforms are typically designed to detect crop features that are native to this environment, such as leaf color, crop type, fruit location, etc. For instance, weed management robots, including AgBot II, detects and classifies weeds to either be chemically or mechanically removed [7]; robust citrus fruit picking in [8], [9] and berry picking in [10], [11] are

made possible by detecting and estimating the location of fruits; autonomous fertilizing in [12] is performed for soil deemed necessary based on soil color. Similarly, commercial platforms perform tasks based on visual information gathered about the crop environment. These platforms include the octocopter AGRAS MG-1P [13], Verdant Robotics [14] platforms, and the See & Spray Ultimate from John Deere [15] and [16] Blue River Technologies, used for precise herbicide and pesticide spraying.

Moreover, the type of platform, *e.g.* aerial or ground, is chosen based on the specific precision agriculture task. Since maize stalks emerge from the soil, a ground robot data gathering system is proposed in [17] to estimate maize plant locations based on LiDAR scans; while BoniRob in [18] was designed for autonomous plant phenotyping as well as disease detection. To perform this task on an individual plant basis, a ground robot with four wheel hub motors and hydraulic components offers flexibility with respect to navigation and changing height positions. On the other hand, aerial platforms are proposed in [19] and [20], for fast yield estimation in orchards. In [21], sorghum biomass is estimated using UAV-based hyperspectral and LiDAR data that covers large regions over a short time. Reviews [22]–[24] cover additional platforms and in greater detail. In our work, we opt for a ground vehicle, as it provides a stable platform necessary for imaging the proposed colorimetric leaf sensors.

Among the ground platforms listed above are those that were specifically designed to operate in 30-inch wide row crops, and are therefore comparable in width to ours, at approximately 15-inch. However, these platforms do not have the on-board imaging capabilities that we have and are heavier, causing additional soil compaction than our platform. For example, P-AgBot [25], which was designed to estimate corn crop heights and stalk diameters, with on-board sensing and manipulation is built upon the Clearpath Jackal [26], which weights 37-lb. TerraSentia, developed in [27], was designed specifically for corn stand counting and phenotyping. While a contribution of their system was their ultra compact and lightweight 3D-printed design, their platform is claimed to weight around 30-lb which is heavier than our 20-lb platform. Additionally, both of the aforementioned platforms do not house the on-board imaging capabilities that are required for our task.

Given the great potential of these novel metasurface-based sensors for the future of precision agriculture, their unique operation, and the challenges of their measurement in an outdoor agricultural setting, it is necessary for us to develop a custom platform and imaging pipeline. The robotic system has therefore been designed and developed for the very specific task of traversing agricultural fields, locating these transparent, passive metasurface-based sensors, and measuring their resonance spectrum. Platforms in prior work may solve vision based tasks, but none of the listed work would be able to solve our leaf sensor localization task, a task made challenging by the transparency of the sensor. To add, the platform we propose is designed to house the necessary on-board sensing, and is lightweight compared to existing

platforms that were built for data gathering in agriculture settings.

III. METHODOLOGY

A. Problem Statement

Given an *a priori* map of row crops from satellite imagery, a ground robot platform is tasked to estimate the position and spectra of N leaf sensors deployed in the row crop environment. We assume that the leaf sensor position provides the robot with a non-obstructed view. With this information, the robot must localize the leaf sensor using an on-board monocular RGB camera and object detector. Using a feature-based mapping from the RGB frame to mirror frame, a motorized mirror is controlled to capture a hyperspectral image and spectra of leaf sensors in the row crop environment.

To solve the task described above, we co-design a system consisting of novel colorimetric leaf sensors and a ground robot platform. The system components are described in more detail in this section.

B. Colorimetric Leaf Sensor

The state-of-the-art, passive, colorimetric leaf sensors consist of optical metasurfaces, which are artificially nanostructured surfaces fabricated via a one-step direct imprint of dielectric nanocrystal inks [5]. The metasurface's sub-wavelength nanostructure geometry is designed such that the peaks in the reflectance spectrum, or resonances, occur in the visible spectral range at ~ 650 nm. This ensures that the sensor's resonances do not overlap with leaves' green color (~ 500 - 570 nm), the high reflectance region in the leaves' reflectance spectrum (~ 700 - 1500 nm) which would contribute to optical noise, and the oxygen and water absorptions in the solar spectrum (~ 750 - 850 nm). The optical metasurfaces can be embedded in adaptive polymers which respond to specific plant stress targets. The adaptive polymers respond to the target stimuli with a change in their dielectric properties, leading to a shift in the highly reflective metasurface resonance [28]. This shift in resonance can be read-out as a color change using a spectrometer in a lab environment, or with a hyperspectral camera in an outdoor environment. These novel passive colorimetric sensors enable a more direct and continuous monitoring of plant stressors compared to existing remote sensing techniques, and are of lower cost and energy requirement and smaller form factor compared to commercial crop sensors, enabling deployment at a large-scale and real-time monitoring of crop health [28]. For the purposes of this work the optical metasurface has been fabricated on a glass substrate without the adaptive polymer, with the focus being the first-time demonstration of the localization of the metasurface sensors by a robotic hyperspectral imaging system and the hyperspectral imaging in outdoor environments.

C. Robot Platform

The BEAST robot shown in Fig. 3 is a lightweight and compact, all-terrain ground robot platform. The motivation

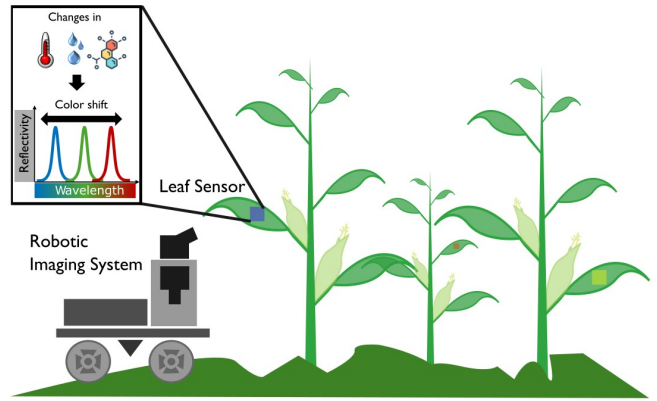


Fig. 2: A schematic of the co-designed sensor and robotic detection system in outdoor row-crop environments.

for this robot is to provide a smaller, lighter, and cheaper alternative to existing agricultural robots. A comparison of the size, weight and cost relative to other platforms is shown in Table I. The high cost and large size of existing agricultural robots pose significant challenges for farmers who must weigh the financial burden and risk crop damage from heavy and invasive machinery. In contrast, the BEAST robot requires minimal financial investment and is able to navigate dense crops while reducing the risk of crop damage and soil-compaction.

TABLE I: Cost and Size Comparison of Agricultural Robots

Robot	Cost	Weight	Footprint
BEAST	$\sim \$3,000$	9kg	480x380mm
Clearpath Jackal	$\sim \$20,000$	17kg	508x430mm
TerraSentia	$\sim \$5,000$	13kg	508x330mm
Clearpath Husky	$> \$20,000$	80kg	990x698mm

The BEAST is equipped with an NVIDIA Jetson Xavier NX processor, designed to be compact with low power consumption. The Jetson contains both a CPU and a GPU for fast image processing, necessary for visual-inertial odometry (VIO) and learning-based object detection for leaf sensor localization. To provide visual-inertial odometry, a Stereolabs Terra AI Zed X is mounted on the front of the robot. The robot is prescribed with a predefined path, and uses waypoint following to autonomously navigate along the path, with all-wheel drive motors and dual-wheel servos to separately control the direction of the front and back wheels. The robot additionally houses a hyperspectral submodule. This is used to acquire hyperspectral images by controlling a motorized mirror to direct light from a region of interest (colorimetric leaf sensor) in a scene onto the hyperspectral camera sensor. This sub-module is described in greater detail in Section III-E. To determine the desired mirror control, the region of interest to capture is determined online by an object detector, identifying colorimetric leaf sensors in images acquired by a FLIR Chameleon3 USB3 RGB camera. This camera is compact and lightweight and outputs a stream of 1.3 megapixel images, providing a balance between image

clarity for object detection and image resolution for timely processing. Finally, to increase the signal-to-noise ratio of the resonance spectra captured by the Hyperspectral camera, a Thorlabs *SLS201L(/M)* Tungsten-Halogen Light Source is mounted and turns on autonomously to illuminate the leaf sensor in the scene during hyperspectral imaging.

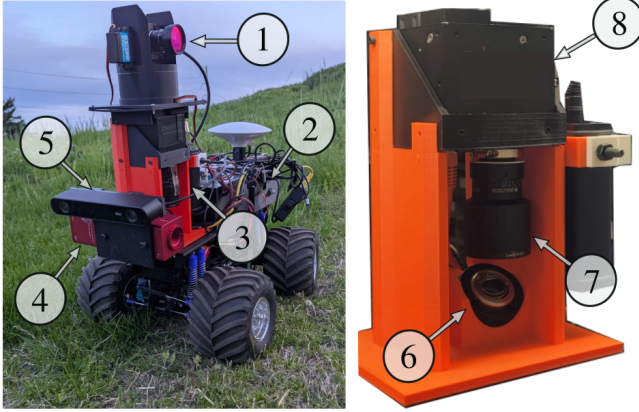


Fig. 3: An overview of the BEAST platform LEFT and close up of hyperspectral sub-module RIGHT. (1) FLIR Chameleon3 RGB camera with pan-tilt mechanism (2) NVIDIA Jetson Xavier NX (3) Hyperspectral sub-module (4) on-board Thorlabs *SLS201L(/M)* Tungsten-Halogen Light Source (5) Stereolabs Terra AI Zed X VIO (6) Optotune Fast Steering Mirror MR-15 – 30–PS 15mm diameter mirror (7) 70 mm focal length lens (8) Headwall Nano-Hyperspec VNIR Imaging Sensor, with spatial resolution of 640p, 400 – 1000nm wavelength, and spectral resolution with 270 bands.

D. Leaf Sensor Detection and Verification

To localize the leaf sensor, we use a YOLOv7 model for object detection [29] with classification confidence. We have opted for YOLOv7 as a lightweight alternative to other object detection models such as [30], for performing inference faster on-board an embedded computer. The model is trained on input-target pairs, where an input is an RGB image of the leaf sensor directly interfacing a plant in the environment, and a target is a human-labeled bounding box representing the size and location of the detected leaf sensor in the given RGB image. Data are acquired with a FLIR Chameleon3 on-board the robot. A total of 2200 images were used for training.

We perform an additional detection verification upon receiving a positive leaf sensor detection. First, at least 3 consecutive positive detections with a small variance in bounding box centroids must be obtained. Then, given the focal length of the hyperspectral camera, known physical size of the leaf sensor and average YOLO bounding box location and size, the robot acquires a hyperspectral image if it calculates that it is within an ideal location for hyperspectral image capture and resonance acquisition, relative to the leaf sensor.

E. Hyperspectral Camera System

In Fig. 3, we show the hyperspectral camera sub-module, which consists of a pushbroom Headwall Nano-Hyperspec visible and near-infrared (VNIR) hyperspectral camera of 400–1000nm 270 bands with spectral resolution of 3nm, and an Optotune Fast Steering MR-15-30-PS 15-mm motorized mirror.

1) *Pushbroom Hyperspectral Camera*: Our camera is an instance of the linear pushbroom model [31]. A pushbroom camera is designed to obtain high spectral resolution images by scanning a target 2D region line by line. For each line scan, light first passes through the camera lens, then through a narrow slit situated at the focal plane of the camera, that corresponds to a line of the scene being imaged.

2) *Motorized Mirror*: While the pushbroom design allows for high spectral resolution images, it comes at the cost of requiring camera motion to capture multiple lines of new information for a 2D image, as well as a narrow field of view (FOV)—limitations that our design overcomes via use of a motorized mirror. To allow for stable motions for the camera mounted on a ground vehicle, instead of moving the robot platform itself to acquire these 2D images, we couple the camera with a motorized mirror, naturally oriented at a 45° angle of incidence to the hyperspectral camera lens. This means that if the mirror is not actuated, it will capture the scene at eye-level with the mirror. However, if the mirror is actuated, assuming the normal vector that originates from the center of the mirror is the axis of reflection, changing the orientation of the mirror changes the angle of reflection. This in turn allows one to choose which part of the scene is reflected onto the mirror, then into the camera. Therefore, this motorized mirror coupled with the hyperspectral camera enables foveation, allowing for high resolution hyperspectral imagery of a selected area within the FOV.

During image capture, the orientation of the motorized mirror is incrementally updated, such that the image acquired represents the target 2D region. For this, we assume that the mirror is large enough to reflect a line that is the size of the hyperspectral camera line width, adopting the same approach as that in [32]. The mirror orientation can be controlled by sending desired tilt angles of the mirror along the x -axis and y -axis. The motorized mirror has a built in PID controller for accurate position feedback control.

We note that given the small size of the leaf sensor (approximately 1-inch. \times 1-inch.), and the focal length of the camera (approximately 40-inch.), it is challenging to locate the leaf sensor by scanning at a coarse line by line resolution, therefore making the prior RGB based leaf detection necessary before performing foveation over the small leaf sensor.

3) *RGB to Motorized Mirror Control*: To determine the area of the scene to scan with the motorized mirror, we estimate the homography between two planes: (1) an image captured by the on-board RGB camera, and (2) the corresponding hyperspectral image of the same scene. The latter is obtained by merging patches of hyperspectral images captured by moving the motorized mirror in tilt angles

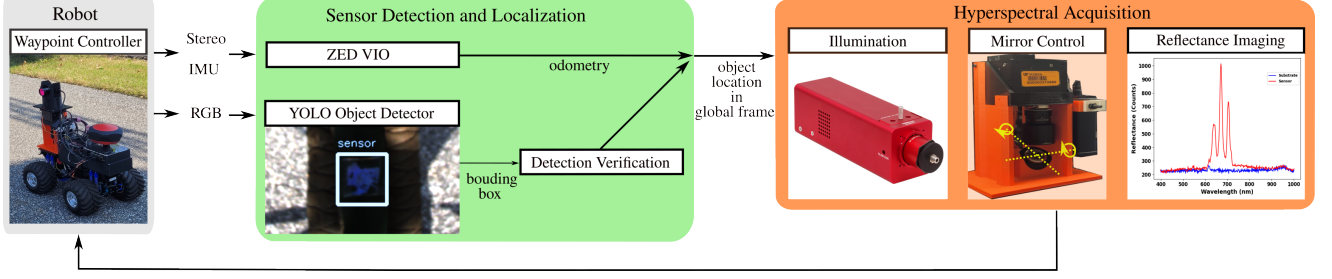


Fig. 4: Full system co-design. A system consisting of metasurface colorimetric leaf sensor; ground robot platform; and hyperspectral imaging submodule.

of the range $[-25^\circ, 25^\circ]$ in both x and y axis. Note that multiple patches are required to obtain the corresponding hyperspectral images, given the small size of one patch of a high resolution image (approximately 2-inch. \times 2-inch.). All of these images are acquired at the focal length of the Hyperspectral camera of approximately 40-inch. We then estimate the homography to estimate the mapping of coordinates in the RGB frame to the motorized mirror tilt angles. Assuming YOLO provides an estimate of the center of the leaf sensor and the size of the bounding box, we use the above mapping to determine the corresponding mirror tilt angles required to sweep over the leaf sensor in the scene.

IV. EXPERIMENTS

A. System Evaluation Metrics

To evaluate the performance of our method, component and system-level testing is conducted in three different experimental settings: (1) Controlled/Structured Indoor Lab Setting, (2) Unstructured Outdoor Setting, and (3) Structured Outdoor Setting. The system-level performance was assessed by the following metrics: (1) YOLO Object detection success in correctly detecting a leaf sensor and causing the robot to take a hyperspectral image of that leaf sensor. (2) Hyperspectral image capture success rate, wherein we quantify the rate at which, once a leaf sensor is detected, a hyperspectral image that successfully captures a portion of that sensor is acquired. (3) Resonance acquisition, where a positive acquisition provides a resonance spectra signal with a noise ratio that is greater than or equal to that in Fig. 9.

B. Structured Indoor Lab Experimental Results

The sensor subsystem's was characterized with a lab spectrometer-based measurement of it's transmission spectrum and angle-dependent transmission spectrum. The full system pipeline is then tested indoors in 22 experiments. The pipeline consists of the following steps: (1) Robot navigation following predefined way points, (2) Object detection and localization of the sensor, (3) Hyperspectral imaging of the localized sensor using a motorized mirror, with halogen lamp illumination, and (4) Resonance spectrum detection from the acquired hyperspectral image. Fig 9 shows the lab spectrometer-measured transmission spectrum compared



Fig. 5: Experiments were conducted in three different settings, an environment (1) indoors and controlled (2), outdoors and unstructured, and (3) outdoors and unstructured. These experiments included runs across different terrains (gravel, soil), and across a total of 5 different days with varying lighting conditions (overcast, partial cloud coverage, and sunny).

with the extracted reflectance spectrum from a hyperspectral image acquired indoors. The resonances are displayed as dips in the spectrometer-measured transmission spectrum, and as peaks in the hyperspectral camera-measured reflectance spectrum. Their spectral locations are closely matched and any difference between the spectrometer and hyperspectral measurement can be attributed to the sensor's diffractive angle dependence, as we show in Fig 9. The angle-dependent transmission measurement shows that the central two resonance modes shift in position and split into higher-order diffractive modes as the angle-of-collection is changed from 0 to 10 degrees. The angle-of-collection with the hyperspectral camera varies with each image acquisition, since the robot location in front of the sensor and the mirror angle varies. Therefore, we see shifts on the order of ≈ 20 nm in

the resonance spectrum with each measurement.

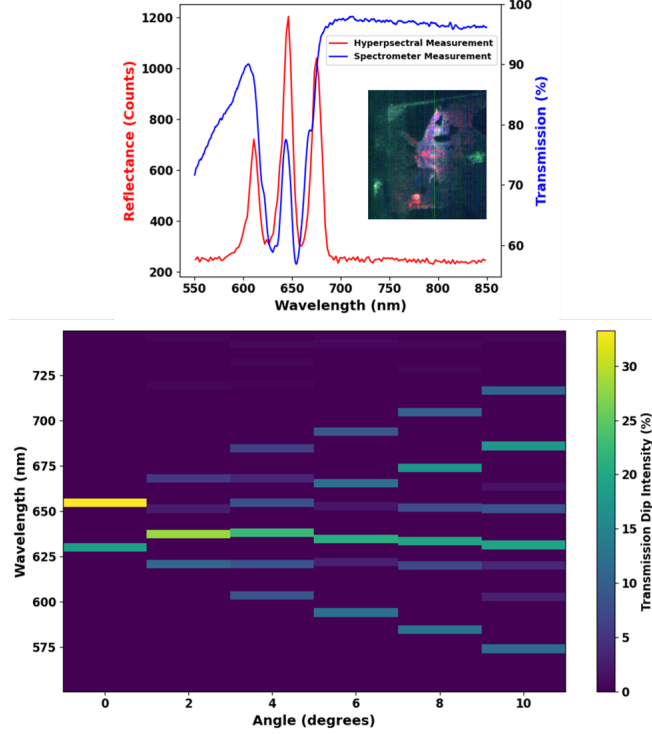


Fig. 6: Indoor characterization of the leaf sensor resonance spectrum TOP using a lab spectrometer and the hyperspectral camera onboard the BEAST during full pipeline testing. BOTTOM using a lab spectrometer to measure its angle dependence transmission spectrum.

Within 22 structured indoor experiments, the system achieved a 77% overall success rate in acquiring a resonance from hyperspectral images of the leaf sensor. The experimental runs that failed included a failed detection for 1 out of 22, and in the remaining 4 runs, while a hyperspectral image was acquired, the resonance’s signal-to-noise ratio was insufficient to be measurable. The signal-to-noise ratio required for successful resonance detection will be discussed in further detail below. It is important to note that the leaf sensor’s location remained consistent in all 22 runs, allowing the robot to be tuned accordingly. This tuning involved programming the robot to slow down upon detecting the leaf sensor within a predefined range in its image view, where resonance acquisition was most likely to succeed. If the sensor location were to change, the robot would require retuning to identify the new range within its image view where resonance acquisition is feasible.

C. Unstructured Outdoor Experimental Results

System-level testing was conducted outdoors to determine the feasibility of detecting leaf sensors and capturing a hyperspectral image of them in an unstructured environment, where both the number of leaf sensors present and the location of leaf-sensor-bearing plants varied. The same pipeline used in the indoor experiments was implemented. However, due to the strict spacial and angular thresholds necessary

for resonance acquisition and the lack of precise plant positioning to account for this, resonance acquisition was not expected in these trials and halogen light functionality was omitted. Ten outdoor unstructured experiments were performed in a row-crop environment consisting of three plant rows, each with two plants capable of bearing a sensor, as depicted in Figure 7. The experiments were categorized into three types based on number and distribution of leaf sensors. Four trials included a single sensor in the first row, three trials included one sensor in the first row and one sensor in the third row, and the remaining three included one sensor in the first row and one sensor in the second row. Across the ten outdoor unstructured experiments, the system achieved 90% success in acquiring hyperspectral images of all present leaf sensors, regardless of plant location.



Fig. 7: Unstructured environment that the BEAST was evaluated in, with example robot trajectory. Colorimetric leaf sensors were mounted on 2 out of 16 plants in the environment.

D. Structured Outdoor Experimental Results

Based on the results of the unstructured outdoor experiments, performed with three plant rows and varying leaf sensor locations, we conducted 10 structured outdoor experiments, where only a single row was used and the plant bearing a leaf sensor was fixed in an ideal position to meet the spatial and angular thresholds required for resonance acquisition. In these ten structured experiments, the system achieved a 100% success rate in acquiring hyperspectral images of the sensor and an 80% success rate in detecting the leaf sensor’s resonance from the acquired hyperspectral images. Figure 9 shows spectra obtained from the experiments where the leaf sensor resonance was acquired. The measured resonances fall within 20 nm of the lab-spectrometer-measured resonance wavelengths, with variation due to variation in the angle of collection.

V. LIMITATIONS

There are a few limitations to the methodology. First, the hyperspectral camera used has a fixed focal length, which restricts it to capturing a resonance from the leaf sensor only at a distance of 1 meter from the lens. Second, the leaf sensor only reflects its resonance within ± 4 degrees

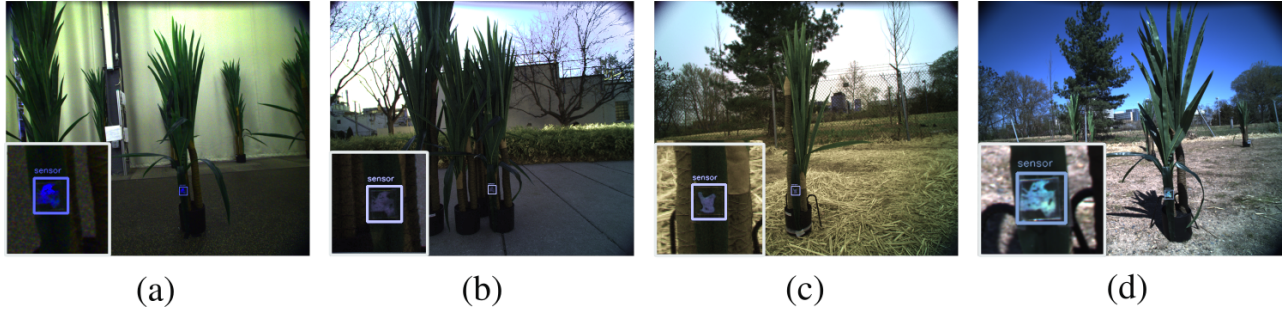


Fig. 8: Successful detections of leaf sensors on unseen data in various settings: indoor (a), semi-structured outdoor (b), unstructured outdoor in overcast conditions (c), and unstructured outdoor in overcast conditions (d). In all figures, we show the environment, and an enlarged image of the successful YOLO bounding box in the bottom left hand corner. Note, the colors have been altered to

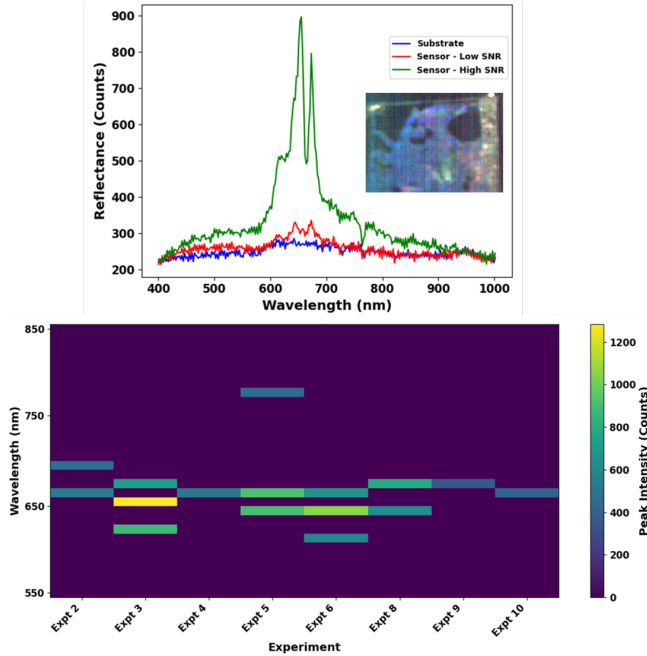


Fig. 9: Outdoor characterization of the leaf sensor resonance spectrum TOP using the hyperspectral camera onboard the BEAST during full pipeline testing. Shows the differences in resonance signal-to-noise ratio in varying imaging conditions. BOTTOM Variation in the measured resonance's spectral position for each experimental run

from the perpendicular direction at a 1-meter distance. Third, because the resonance requires perpendicular acquisition, the specific leaf that carries the leaf sensor on a plant must be fixed in such a way that it remains perpendicular to the robot's trajectory within the row and at predetermined height. The combination of these 3 constraints require the robot to precisely navigate to a $76 \times 25 \text{ mm}$ area, located $914 \text{ mm} \pm 25 \text{ mm}$ away from the leaf sensor and aligned perpendicular to it, or else a resonance cannot be captured. The robot is tuned to ignore leaf sensor detections that are outside of this specific threshold within its view. Lastly, we do not implement functionality for the robot to reposition to be

	Precision	Recall	mAP@0.5	mAP@.5:.95
Yolov7	99.3	99.3	99.1	82.8
Yolov11n	99.2	99.3	99.3	82.1
Yolov11x	99.2	99.3	99.3	83.8
Yolov10n	99.2	99.3	98.9	82.1

TABLE II: YOLO results on the training set, with RGB images where the leaf sensor is positioned at a variety of distances and angles from the RGB camera. We report on the precision, recall, and mean average precision (mAP) statistics.

perpendicular to the leaf sensor based on leaf sensor depth and angle estimation. Thus, if the robot makes an error during navigation, causing it to no longer be positioned straight, it will be unable to capture a resonance.

VI. CONCLUSIONS

In this work, we co-design a novel leaf sensor and a ground robot platform system towards acquiring direct plant stress indicators for actionable information for farmers. The leaf sensors are designed to measure plant health more directly than existing remote sensing technologies, as this leaf sensor makes direct contact with the surface of the plant. As the manufacturing cost of these leaf sensors decreases, we envision being able to obtain direct, high-resolution crop health measurements, allowing for higher-quality decision making by farmers, and the employment of more precise farming technologies.

While the results shown in this work are promising, we have identified some interesting directions for future work. Given the precision of robot pose required to capture a hyperspectral image and spectra from a fixed focal lens camera, in future work, we plan to develop a variable focal lens that can adapt its focus based on the distance between the hyperspectral camera and the colorimetric leaf sensor. We also plan to increase the precision of robot control. In addition, we plan to design and manufacture colorimetric leaf sensors with a higher signal-to-noise ratio. Finally, to further reduce false positive detections, instead of performing object detection on full RGB images, we plan to segment foliage

or plants, and perform colorimetric leaf detection on these segmented regions.

ACKNOWLEDGEMENT

We gratefully acknowledge the support provided by the Internet of Things for Precision Agriculture (IoT4Ag) NSF ERC Grant EEC-1941529.

REFERENCES

- [1] D. J. Mulla, "Twenty five years of remote sensing in precision agriculture: Key advances and remaining knowledge gaps," *Biosystems engineering*, vol. 114, no. 4, pp. 358–371, 2013.
- [2] M. Weiss, F. Jacob, and G. Duveiller, "Remote sensing for agricultural applications: A meta-review," *Remote sensing of environment*, vol. 236, p. 111402, 2020.
- [3] X. Guo, "Surface plasmon resonance based biosensor technique: a review," *Journal of biophotonics*, vol. 5, no. 7, pp. 483–501, 2012.
- [4] P. Wu, S. Qu, X. Zeng, N. Su, M. Chen, and Y. Yu, "High-q refractive index sensors based on all-dielectric metasurfaces," *RSC advances*, vol. 12, no. 33, pp. 21264–21269, 2022.
- [5] A. Mallavarapu, C. F. Lawrence, B. Huang, B. O. Maldonado, P. Arratia, and C. R. Kagan, "Tio2 metasurfaces with visible quasi-guided mode resonances via direct imprinting of aqueous nanocrystal dispersions," *ACS Applied Nano Materials*, vol. 6, no. 18, pp. 17294–17300, 2023.
- [6] A. Garg, S. Bordoloi, S. P. Ganesan, S. Sekharan, and L. Sahoo, "A relook into plant wilting: observational evidence based on unsaturated soil–plant–photosynthesis interaction," *Scientific Reports*, vol. 10, no. 1, p. 22064, 2020.
- [7] O. Bawden, D. Ball, J. Kulk, T. Perez, and R. Russell, "A lightweight, modular robotic vehicle for the sustainable intensification of agriculture," in *Proceedings of the 16th Australasian Conference on Robotics and Automation 2014*, pp. 1–9, Australian Robotics and Automation Association (ARAA), 2014.
- [8] S. Mehta and T. Burks, "Vision-based control of robotic manipulator for citrus harvesting," *Computers and electronics in agriculture*, vol. 102, pp. 146–158, 2014.
- [9] S. S. Mehta, W. MacKunis, and T. F. Burks, "Robust visual servo control in the presence of fruit motion for robotic citrus harvesting," *Computers and Electronics in Agriculture*, vol. 123, pp. 362–375, 2016.
- [10] Y. Xiong, C. Peng, L. Grimstad, P. J. From, and V. Isler, "Development and field evaluation of a strawberry harvesting robot with a cable-driven gripper," *Computers and electronics in agriculture*, vol. 157, pp. 392–402, 2019.
- [11] N. K. Uppalapati, B. Walt, A. J. Havens, A. Mahdian, G. Chowdhary, and G. Krishnan, "A berry picking robot with a hybrid soft-rigid arm: Design and task space control," in *Robotics: Science and Systems*, p. 95, 2020.
- [12] R. N. Bhimanpallewar and M. R. Narasingarao, "Agrirobot: implementation and evaluation of an automatic robot for seeding and fertiliser microdosing in precision agriculture," *International Journal of Agricultural Resources, Governance and Ecology*, vol. 16, no. 1, pp. 33–50, 2020.
- [13] DJI, "AGRAS MG-1P SERIES: Innovative Insights. Increased Efficiency." <https://www.dji.com/br/mg-1p>. Accessed on 1 March 2024.
- [14] Verdant Robotics, "Product 1." <https://www.verdantrobotics.com/product-1>. Accessed on 1 March 2024.
- [15] John Deere, "See & Spray Ultimate." <https://www.deere.com/en/news/all-news/see-spray-ultimate/>. Accessed on 1 March 2024.
- [16] Blue River Technology, "Our Products." <https://bluerivertechnology.com/our-products/>. Accessed on 1 March 2024.
- [17] U. Weiss and P. Biber, "Plant detection and mapping for agricultural robots using a 3d lidar sensor," *Robotics and autonomous systems*, vol. 59, no. 5, pp. 265–273, 2011.
- [18] A. Ruckelshausen, P. Biber, M. Dorna, H. Gremmes, R. Klose, A. Linz, R. Rahe, R. Resch, M. Thiel, D. Trautz, et al., "Bonirob: an autonomous field robot platform for individual plant phenotyping," in *Precision agriculture'09*, pp. 841–847, Wageningen Academic, 2009.
- [19] S. W. Chen, S. S. Shivakumar, S. Dcunha, J. Das, E. Okon, C. Qu, C. J. Taylor, and V. Kumar, "Counting apples and oranges with deep learning: A data-driven approach," *IEEE Robotics and Automation Letters*, vol. 2, no. 2, pp. 781–788, 2017.
- [20] X. Liu, S. W. Chen, S. Aditya, N. Sivakumar, S. Dcunha, C. Qu, C. J. Taylor, J. Das, and V. Kumar, "Robust fruit counting: Combining deep learning, tracking, and structure from motion," in *2018 IEEE/RSJ international Conference on intelligent robots and systems (IROS)*, pp. 1045–1052, IEEE, 2018.
- [21] A. Masjedi, M. M. Crawford, N. R. Carpenter, and M. R. Tuinstra, "Multi-temporal predictive modelling of sorghum biomass using uav-based hyperspectral and lidar data," *Remote Sensing*, vol. 12, no. 21, p. 3587, 2020.
- [22] R. R. Shamsheeri, C. Weltzien, I. A. Hameed, I. J. Yule, T. E. Grift, S. K. Balasundram, L. Pitonakova, D. Ahmad, and G. Chowdhary, "Research and development in agricultural robotics: A perspective of digital farming," 2018.
- [23] L. F. Oliveira, A. P. Moreira, and M. F. Silva, "Advances in agriculture robotics: A state-of-the-art review and challenges ahead," *Robotics*, vol. 10, no. 2, p. 52, 2021.
- [24] C. Cheng, J. Fu, H. Su, and L. Ren, "Recent advancements in agriculture robots: Benefits and challenges," *Machines*, vol. 11, no. 1, p. 48, 2023.
- [25] K. Kim, A. Deb, and D. J. Cappelleri, "P-agbot: In-row & under-canopy agricultural robot for monitoring and physical sampling," *IEEE Robotics and Automation Letters*, vol. 7, no. 3, pp. 7942–7949, 2022.
- [26] Clearpath Robotics, "Jackal Small Unmanned Ground Vehicle." <https://clearpathrobotics.com/jackal-small-unmanned-ground-vehicle/>. Accessed on 16 March 2024.
- [27] E. Kayacan, Z.-Z. Zhang, and G. Chowdhary, "Embedded high precision control and corn stand counting algorithms for an ultra-compact 3d printed field robot," in *Robotics: science and systems*, vol. 14, p. 9, 2018.
- [28] W. Chen, G. Wu, M. Zhang, N. J. Greybush, J. P. Howard-Jennings, N. Song, F. Stinner, S. Yang, and C. R. Kagan, "Tio2 metasurfaces with visible quasi-guided mode resonances via direct imprinting of aqueous nanocrystal dispersions," *ACS Applied Nano Materials*, vol. 1, no. 3, pp. 1430–1437, 2018.
- [29] C.-Y. Wang, A. Bochkovskiy, and H.-Y. M. Liao, "Yolov7: Trainable bag-of-freebies sets new state-of-the-art for real-time object detectors," in *Proceedings of the IEEE/CVF conference on computer vision and pattern recognition*, pp. 7464–7475, 2023.
- [30] S. Ren, K. He, R. Girshick, and J. Sun, "Faster r-cnn: Towards real-time object detection with region proposal networks," *Advances in neural information processing systems*, vol. 28, 2015.
- [31] R. Gupta and R. I. Hartley, "Linear pushbroom cameras," *IEEE Transactions on pattern analysis and machine intelligence*, vol. 19, no. 9, pp. 963–975, 1997.
- [32] B. Tilmon, E. Jain, S. Ferrari, and S. Koppal, "FoveaCam: A MEMS mirror-enabled foveating camera," in *2020 IEEE International Conference on Computational Photography (ICCP)*, pp. 1–11. ISSN: 2472-7636.